Vol 18 No 5, May 2009
1674-1056/2009/18(05)/1961-07

Chinese Physics B

© 2009 Chin. Phys. Soc.
and IOP Publishing Ltd

$4f^{N-1}5d$ energy levels of lanthanides: a quasi-angular-momentum approach and its application to $Cs_2NaYF_6:Er^{3+}$*

Ma Chong-Geng(马崇庚)[a], Jiang Sha(江 莎)[a], Duan Chang-Kui(段昌奎)[a]†, Yin Min(尹 民)[b], and Xia Shang-Da(夏上达)[a][b]

[a] *Institute of Modern Physics, Chongqing University of Post and Telecommunications, Chongqing 400065, China*

[b] *Department of Physics and Hefei National Laboratory for Physical Science at Microscale, University of Science and Technology of China, Hefei 230026, China*

(Received 12 October 2008; revised manuscript received 6 November 2008)

The spin–orbit interaction of the 5d electron needs to be taken into account to give the proper energy structure for the $4f^{N-1}5d$ configuration of heavy lanthanide ions occupying a site with ligands forming an octahedron. This paper derives theoretical results for the energy structure by treating the t_2 orbitals as quasi p orbitals and then using angular-momentum coupling techniques. An analytic expression for the electric dipole absorption line strengths between $4f^N$ multiplets and $4f^{N-1}5d$ states is given in terms of various angular-momentum quantum numbers and re-coupling coefficients. The result is then applied to interpret the excitation spectrum of $Cs_2NaYF_6:Er^{3+}$. The high-spin and low-spin states of $Cs_2NaYF_6:Er^{3+}$ are discussed in terms of the wavefunctions obtained by using the developed theoretical model.

Keywords: f–d transition, octahedral site, spin–orbit interaction, coupling of angular momenta
PACC: 7115, 7170C, 7630K, 7840

1. Introduction

Due to the need for new ultraviolet (UV) and vacuum-ultra-violet (VUV) phosphors, scintillators, and lasers, and the requirements for applications in white light electric diodes, plasma display panels, mercury-free fluorescent tubes etc., there have been many studies in recent years, which aimed at extending the fundamental knowledge of the high-energy $4f^N$-$4f^{N-1}5d$ transition (hereafter referred to as the f–d transition) of lanthanide ions doped in crystals.[1–16] The availability of UV and VUV synchrotron radiation has been an important impetus in these studies.

The semi-empirical calculations of energy levels for the $4f^N$ configuration have been extended to the $4f^{N-1}5d$ configuration[3] and extensive calculations have been carried out for trivalent lanthanide ions in crystals, which give satisfactory agreement with experimental f–d spectra of lanthanide ions in YPO_4, CaF_2 and $LiYF_4$ hosts.[4,17] However, such calculations usually involve dozens of adjustable parameters and predict hundreds or thousands of electronic transition lines to be convolved into several to a few dozen broad bands. In comparison, there are very limited (several to a few dozen at most) peaks in measured absorption or excitation spectra. Hence, a simplified calculation (hereafter referred to as the simple model) involving 2–3 adjustable parameters has been developed by adopting various approximations, such as omitting weak interactions.[18,19]

The simple model[18,19] ignored the 5d spin–orbit interaction for simplicity, and has been applied to those systems where the approximation is appropriate. However, for heavy lanthanide ions in octahedral six-fold coordination compounds, where the measured spectra involve the low-lying t_2 component of 5d orbitals with orbital angular momentum not fully quenched, the splitting caused by the 5d spin–orbit interaction can be as much as a few thousand wave numbers. Hence, it is necessary to include the 5d spin–orbit interaction in this octahedral case.

In this work, we take the 5d spin–orbit interaction into account in the simple model by treating t_2 orbitals as equivalent p orbitals. The energy levels and line strengths are derived by utilizing Racah–Wigner algebra.[20] The theoretical developments are

*Project supported by the National Natural Science Foundation of China (Grant Nos 10874173 and 10774140).
†Corresponding author. E-mail: duanck73@hotmail.com

applied to interpret the f–d excitation spectrum of Cs_2NaYF_6:Er^{3+} by referring to the Dieke diagram and resorting to very limited numerical calculations.

2. Theory

2.1. Approximate Hamiltonian and energy level structure for the $4f^{N-1}5d$ configuration

The Hamiltonian for the $4f^{N-1}5d$ configuration can be written as

$$\begin{aligned} H(4f^{N-1}5d) = & H_{\rm Coul}({\rm ff}) + H_{\rm cf}({\rm d}) \\ & + H_{\rm so}({\rm f}) + H_{\rm Coul}({\rm fd}) \\ & + H_{\rm so}({\rm d}) + H_{\rm cf}({\rm f}). \end{aligned} \tag{1}$$

The first two terms (i.e., the Coulomb interaction between 4f electrons and the crystal–field interaction for the 5d electron) are the strongest interactions. We shall denote the sum of these two terms as H_0. The eigenstate of H_0 is the product of the $4f^{N-1}\eta_{\rm f}S_{\rm f}L_{\rm f}$ spectral term of $4f^{N-1}$ configuration with the ${}^2\Gamma_{\rm d}$ crystal–field component of 5d electron, i.e., $(4f^{N-1}\eta_{\rm f}S_{\rm f}L_{\rm f}, {}^2\Gamma_{\rm d})$, which forms a subspace. The corresponding eigenvalue energy is the sum of the term energy $E_0(4f^{N-1}\eta_{\rm f}S_{\rm f}L_{\rm f})$ for $4f^{N-1}\eta_{\rm f}S_{\rm f}L_{\rm f}$ and the crystal–field splitting energy $\varepsilon(\Gamma_{\rm d})$ for ${}^2\Gamma_{\rm d}$, i.e.,

$$E_0(4f^{N-1}\eta_{\rm f}S_{\rm f}L_{\rm f},{}^2\Gamma_{\rm d}) = E_0(4f^{N-1}\eta_{\rm f}S_{\rm f}L_{\rm f}) + \varepsilon(\Gamma_{\rm d}). \tag{2}$$

The third term $H_{\rm so}$(f) of Eq.(1) is the spin–orbit interaction for 4f electrons. It can be approximated within the $\eta_{\rm f}S_{\rm f}L_{\rm f}$ spectral term for $4f^{N-1}$ configuration as[21]

$$H_{\rm so}({\rm f}) = \sum_{i=1,\ldots,N} \zeta_{4{\rm f}} \boldsymbol{s}_i \cdot \boldsymbol{l}_i \approx \lambda_{\eta_{\rm f}S_{\rm f}L_{\rm f}} \boldsymbol{S}_{\rm f} \cdot \boldsymbol{L}_{\rm f}. \tag{3}$$

For the $\eta_{\rm f}S_{\rm f}L_{\rm f}$ with the largest possible $S_{\rm f}$,

$$\lambda_{\eta_{\rm f}S_{\rm f}L_{\rm f}} = {\rm sign}(8-N)\zeta_{4{\rm f}}/2S_{\rm f}. \tag{4}$$

The fourth term $H_{\rm Coul}$(fd) of Eq.(1) is the Coulomb interaction between 4f and 5d electrons. In the subspace $(4f^{N-1}\eta_{\rm f}S_{\rm f}L_{\rm f},\ {}^2\Gamma_{\rm d})$, it can be approximated as[18]

$$H_{\rm ex}({\rm fd}) = -J_{\rm ex}\boldsymbol{S}_{\rm f} \cdot \boldsymbol{s}_{\rm d}, \tag{5}$$

where

$$\begin{aligned} J_{\rm ex} = & \frac{6}{35}G^1({\rm fd}) + \frac{8}{105}G^3({\rm fd}) \\ & + \frac{20}{231}G^5({\rm fd}). \end{aligned} \tag{6}$$

The fifth term $H_{\rm so}$(d) of Eq.(1) was previously ignored in the simple model[18,19] since it usually does not cause splitting of $\Gamma_{\rm d}$. However, $H_{\rm so}$(d) can split t_2 components of 5d orbitals and this is no longer negligible for heavy lanthanide ions due to the large $\zeta_{5{\rm d}}$ value. It has been shown[22,23] that the t_2 orbitals can be treated as equivalent p orbitals, i.e.,

$$H_{\rm so}({\rm d}) = \zeta_{5{\rm d}}\boldsymbol{s}_{\rm d}\cdot\boldsymbol{1}_{\rm d} \approx \zeta_{5{\rm d}}\boldsymbol{s}_{\rm d}\cdot\boldsymbol{1}_{{\rm t}_2} = -\zeta_{5{\rm d}}\boldsymbol{s}_{\rm d}\cdot\boldsymbol{1}_{\rm p}, \tag{7}$$

where $\boldsymbol{1}_{\rm t2}$ is the truncation of the $\boldsymbol{1}_{\rm d}$ angular-momentum operator into the space of t_2 orbitals, and $\boldsymbol{1}_{\rm p}$ is the angular-momentum operator acting on the space of p orbitals. We have used $\boldsymbol{1}_{\rm t2} = -\boldsymbol{1}_{\rm p}$[23] in the derivation. The last term $H_{\rm cf}$(f) of Eq.(1) is the crystal–field interaction felt by the 4f electrons. This term is usually very weak and can only cause the splitting of smaller or comparable to the energy of an optical phonon. Such splitting is seldom resolved experimentally, and so $H_{\rm cf}$(f) is ignored here.

Hence, for heavy lanthanide ions in octahedral sites, we shall use the extended simple model[21] for the higher energy $4f^{N-1}(5de_g)$ states and the following effective Hamiltonian $H_{\rm eff}[4f^{N-1}(5dt_2)]$ for the lower energy $4f^{N-1}(5dt_2)$ states, i.e.,

$$\begin{aligned} & H_{\rm eff}\left[4f^{N-1}(5dt_{2g})\right] \\ = & H_0 + \lambda_{\eta_{\rm f}S_{\rm f}L_{\rm f}}\boldsymbol{S}_{\rm f}\cdot\boldsymbol{L}_{\rm f} \\ & - J_{\rm ex}\boldsymbol{S}_{\rm f}\cdot\boldsymbol{s}_{\rm d} - \zeta_{5{\rm d}}\boldsymbol{s}_{\rm d}\cdot\boldsymbol{1}_{\rm p}. \end{aligned} \tag{8}$$

A (quasi-) total angular momentum can be defined as

$$\boldsymbol{J}_{\rm tp} = \boldsymbol{S}_{\rm f} + \boldsymbol{s}_{\rm d} + \boldsymbol{L}_{\rm f} + \boldsymbol{1}_{\rm p}. \tag{9}$$

It is straightforward to verify that $\boldsymbol{J}_{\rm tp}$ has the properties of an angular momentum operator since it is the sum of four independent angular momentum operators. It is noted that $\boldsymbol{J}_{\rm tp}$ is not the actual total angular momentum operator for the $4f^{N-1}5d$ system. It can be seen that $\boldsymbol{J}_{\rm tp}$ commutes with $H_{\rm eff}$, and so the quantum numbers ($J_{\rm tp}$ for the $\boldsymbol{J}_{\rm tp}^2$ and $M_{\rm tp}$ for the z-component $(\boldsymbol{J}_{\rm tp})_z$) may be used to characterize the eigenstates of $H_{\rm eff}$.

Angular momentum operators $\boldsymbol{J}_{\rm f} = \boldsymbol{S}_{\rm f} + \boldsymbol{L}_{\rm f}$ and $\boldsymbol{J} = \boldsymbol{J}_{\rm f} + \boldsymbol{s}_{\rm d}$ do not commute with $H_{\rm eff}$. Nevertheless, since $\boldsymbol{J}_{\rm f}^2$, $\boldsymbol{J}^2$, $\boldsymbol{J}_{\rm tp}^2$ and $((\boldsymbol{J}_{\rm tp})_z)$ mutually commute, their quantum numbers may be used to classify the basis for $4f^{N-1}(5dt_2)$. Here for heavy trivalent lanthanide ion, such as Er^{3+}, the strength of interactions follows $H_{\rm so}({\rm f}) > H_{\rm ex}({\rm fd}) > H_{\rm so}({\rm d})$, so that the coupling scheme $((SO_3^{S_{\rm f}} \times SO_3^{L_{\rm f}}) \times SO_3^{s_{\rm d}}) \times SO_3^{1_{\rm p}}$ may be preferred. Without taking into account the mixing of basis in the eigenstates, the eigenstate can be

approximated as $|[(4f^{N-1}\eta_f S_f L_f J_f,\ s_d)J,\ l_p]J_{tp}M_{tp}\rangle$. Following the same procedure of Ref.[21], we can give its eigenvalue as

$$\begin{aligned}
&E\left(\left|\left[(4f^{N-1}\eta_f S_f L_f J_f, s_d)J, l_p\right] J_{tp}M_{tp}\right\rangle\right)\\
&=\left[E_0\left(4f^{N-1}\eta_f S_f L_f\right)+\varepsilon(t_2)\right]\\
&\quad+\frac{\lambda_{\eta_f S_f L_f}}{2}[J_f(J_f+1)\text{ - }S_f(S_f+1)\text{ - }L_f(L_f+1)]\\
&\quad-J_{ex}\frac{J_f(J_f+1)+S_f(S_f+1)-L_f(L_f+1)}{2J_f(J_f+1)}\\
&\quad\times\frac{J(J+1)-J_f(J_f+1)-s_d(s_d+1)}{2}\\
&\quad-\zeta_{5d}\frac{J(J+1)+3/4-J_f(J_f+1)}{2J(J+1)}\\
&\quad\times\frac{J_{tp}(J_{tp}+1)-J(J+1)-2}{2}. \qquad (10)
\end{aligned}$$

Here $J_f=|L_f-S_f|, |L_f-S_f+1|, \ldots, L_f+S_f$ is the quantum number for $\boldsymbol{J}_f^2$, $J=J_f\pm 1/2$ (or only one value $1/2$ when $J_f=0$) is that for $\boldsymbol{J}^2$, and $J_{tp}=J-1$, J and $J+1$ (or two values J and $J+1$ when $J=0$ or $1/2$) is that for $\boldsymbol{J}_{tp}^2$. The first to the fourth terms in Eq.(10) are the contributions due to H_0, $H_{so}(f)$, $H_{ex}(fd)$ and $H_{so}(d)$, respectively. It is viable to improve the second term of Eq.(10) by using more accurate splitting of multiplets for the ion with $4f^{N-1}$ configuration given in the Dieke diagram. In doing so, a proper scaling is required by using a ratio of ζ_{4f} for $4f^{N-1}5d$ configuration (say, Er^{3+}) against the value for the ion with $4f^{N-1}$ configuration (say, Ho^{3+}). Hence, we use

$$\begin{aligned}
&E\left(\left|\left[(4f^{N-1}\eta_f S_f L_f J_f, s_d)J, l_p\right] J_{tp}M_{tp}\right\rangle\right)\\
&=\varepsilon(t_2)+E(4f^{N-1}\eta_f S_f L_f J_f)\\
&\quad-J_{ex}\frac{J_f(J_f+1)+S_f(S_f+1)-L_f(L_f+1)}{2J_f(J_f+1)}\\
&\quad\times\frac{J(J+1)-J_f(J_f+1)-s_d(s_d+1)}{2}\\
&\quad-\zeta_{5d}\frac{J(J+1)+3/4-J_f(J_f+1)}{2J(J+1)}\\
&\quad\times\frac{J_{tp}(J_{tp}+1)-J(J+1)-2}{2}. \qquad (11)
\end{aligned}$$

Here $E(4f^{N-1}\eta_f S_f L_f J_f)$ is read off from the Dieke diagram and scaled up slightly, and $\varepsilon(t_2)$ is then estimated from the 5d crystal–field splitting for Ce^{3+} in the same host (by scaling down slightly due to the reduction of crystal–field strength).

It is desirable to do a diagonalization of $H_{eff}[4f^{N-1}(5dt_2)]$ in the subspace $(4f^{N-1}\eta_f S_f L_f,\ ^2\Gamma_d)$ for more accurate energies. This requires the matrix elements of $H_{ex}(fd)$ and $H_{so}(d)$ between states

$$|\psi\rangle=\left|\left[(4f^{N-1}\eta_f S_f L_f J_f, s_d)J, l_p\right] J_{tp}M_{tp}\right\rangle \qquad (12)$$

and

$$|\psi'\rangle=\left|\left[(4f^{N-1}\eta_f S_f L_f J'_f, s_d)J', l_p\right] J_{tp}M_{tp}\right\rangle. \qquad (13)$$

Those matrix elements can be derived by using Racah–Wigner algebra (here using explicitly Eqs.(11.47), (11.20) and (11.39) in Ref.[20]). This is complicated but straightforward. The resultant matrix elements are

$$\begin{aligned}
&\langle\psi|\,H_{ex}(fd)\,|\psi'\rangle\\
&=(-J_{ex})\delta_{J,J'}\\
&\quad\times(-1)^{L_f+S_f-J+\frac{1}{2}}\cdot\sqrt{[J_f][J'_f][S_f]S_f(S_f+1)}\\
&\quad\times\cdot\sqrt{\frac{3}{2}}\cdot\left\{\begin{array}{ccc} J_f & s_d & J\\ s_d & J'_f & 1\end{array}\right\}\cdot\left\{\begin{array}{ccc} S_f & L_f & J_f\\ J'_f & 1 & S_f\end{array}\right\}, \qquad (14)
\end{aligned}$$

and

$$\begin{aligned}
&\langle\psi|\,H_{so}(d)\,|\psi'\rangle\\
&=(-\varsigma_{5d})\cdot\langle\psi|\,\boldsymbol{s}_d\cdot\boldsymbol{l}_p\,|\psi'\rangle\\
&=\delta_{J_f,J'_f}\cdot\varsigma_{5d}\cdot(-1)^{1+J_f+s_d+J+J'+J_{tp}}\\
&\quad\times 3\sqrt{[J]\,[J']}\left\{\begin{array}{ccc} J & l_p & J_{tp}\\ l_p & J' & 1\end{array}\right\}\left\{\begin{array}{ccc} J_f & s_d & J\\ 1 & J' & s_d\end{array}\right\}. \qquad (15)
\end{aligned}$$

The symbol such as $[J]=2J+1$ is the dimension of the space with angular momentum J. The curly brackets $\{\ldots\}$ containing 6 angular-momentum quantum numbers are $6j$ symbols.[24]

Since the interactions are independent of M_{tp}, and J_{tp} is a good quantum number, we need only construct a small matrix for each J_{tp} (and an arbitrary given $\text{abs}(M_{tp})\le J_{tp}$) and do the diagonalization.

2.2. Relative line strengths for 4f-5d transitions

The line strength for the electric dipole transition involving isotropic radiation between energy levels of $4f^N$ and $4f^{N-1}5d$ configurations can be written as

$$\begin{aligned}
&S\left[\eta'S'L'J'\leftrightarrow((\eta_f S_f L_f J_f, s_d)J, l_p)J_{tp}\right]\\
&=\frac{1}{3}\sum_{M'M_{tp}m}\left|\left\langle 4f^N\eta'S'L'J'M'\,\left|\boldsymbol{D}^1_m\right|\,\psi\right\rangle\right|^2. \qquad (16)
\end{aligned}$$

The above treatment of t_2 orbitals as quasi p orbitals, however, complicates the calculation of the line strength. The simplification process of Eq.(16) makes use overwhelmingly of group coupling and recoupling techniques and will be presented elsewhere. Here we shall give the final result only as:

$$S = 3N[J_{\rm f}][S'][J_{\rm tp}][J][L'][J'] \times \left|\left\langle 4f^N \eta' S' L' \left\{ \left| 4f^{N-1} \eta_{\rm f} S_{\rm f} L_{\rm f} \right\rangle \right|^2 |\langle 4f\,|r|\,5d\rangle|^2 \right.$$
$$\times \left(\left\{ \begin{array}{ccc} S_{\rm f} & L_{\rm f} & J_{\rm f} \\ J & s_{\rm d} & S' \end{array} \right\} \left\{ \begin{array}{ccc} 3 & L_{\rm f} & L' \\ S' & J' & J \end{array} \right\} \right)^2 \times \sum_{J_t=|J'-1|}^{J'+1} \left([J_t] \left(\left\{ \begin{array}{ccc} 3 & J_t & J_{\rm tp} \\ J & 1 & 2 \end{array} \right\} \left\{ \begin{array}{ccc} J & 3 & J' \\ 1 & J_t & 2 \end{array} \right\} \right)^2 \right) \qquad (17)$$

where $\langle 4f|r|5d\rangle$ is a radial integral, and $\langle 4f^N \eta' S' L' \{|4f^{N-1} \eta_{\rm f} S_{\rm f} L_{\rm f}\rangle$ is the coefficient of fractional parentage given in Ref.[25]. Three angular momentum selection rules $|L' - L_{\rm f}| \leq 3 \leq L' + L_{\rm f}$, $|J' - J| \leq 3 \leq J' + J$ and $|S' - S_{\rm f}| \leq 1/2 \leq S' + S_{\rm f}$, can be derived from the $6j$ symbols in Eq.(17).

3. Application to Er^{3+} in Cs_2NaYF_6

The low-temperature f–d excitation spectrum of the cubic elpasolite Cs_2NaYF_6 crystal doped with Er^{3+} ion has been measured by Makhov *et al.*[26] We choose this as an example for our investigation using the formulae in Section 2. Since the elpasolite host Cs_2NaYF_6 provides a site of octahedral symmetry for the heavy lanthanide ion Er^{3+} to reside in, the component $^2t_2$ of the 5d electron lies lower than the other component ^2e. As shown in the Fig.6 of Ref.[26] and also Fig.1 here, the f–d excitation spectrum contains seven broad bands with maxima at 162.4 nm (A), 155.5 nm (B), 147.2 nm (C), 145.5 nm (D), 135.8 nm (E), 126.2 nm (F) and 120.9 nm (G). The five bands A to E are assigned to transitions to the levels with the 5d electron falling in $^2t_2$ orbitals. The other two bands F and G are assigned to the transitions to the levels with the 5d electron in ^2e orbitals, since the thus-assigned splitting between e and t_2 levels is similar to the splitting of $\sim 18.2 \times 10^3$ cm^{-1} for the 5d orbitals of Ce^{3+} in a similar elpasolite Rb_2NaYF_6.[27]

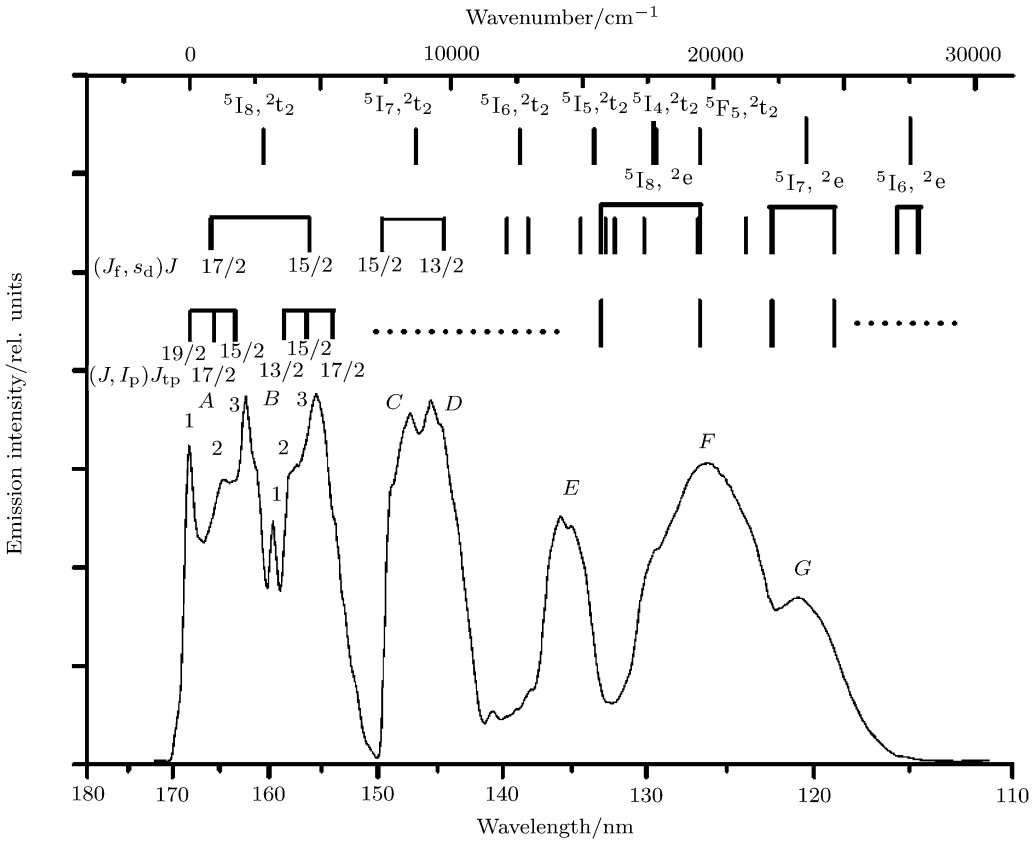


Fig.1. Assignments of the excitation spectrum of Er^{3+} in Cs_2NaYF_6 measured by Makhov *et al.* (Ref.[26]). Note The calculations are described in detail in Section 3; the energy (in units of cm^{-1}) for the A_1 zero-phonon line at 168.1 nm is set as 0 cm^{-1} in the energy axis for the sake of better displaying of splitting between observed peaks.

The position of the seven bands can be calculated by using the formulae in Section 2. We present the energy schemes in Fig.2 by turning on the interactions one by one following the order of strength $H_{so}(f) > H_{ex}(fd) > H_{so}(d)$. By referring to the Dieke diagram and scaling the energy values of the multiplets for $4f^{10}$ configuration up slightly (or alternatively, a free-ion calculation using about 1.06 times of the electrostatic and spin–orbit parameter values listed in Table 3 of Ref.[28], with 1.06 being the Er^{3+} ratio from *ab initio* calculation),[29] we obtain the splitting due to $H_{so}(f)$ as shown in the second column of Fig.2, or numerically, 0 cm^{-1}, 5.8×10^3 cm^{-1}, 9.8×10^3 cm^{-1}, 12.6×10^3 cm^{-1},15.0×10^3 cm^{-1} and 16.7×10^3 cm^{-1} for $^5I_8$, $^5I_7$, $^5I_6$, $^5I_5$, $^5I_4$, $^5F_5$, respectively. The splitting due to $H_{ex}(fd)$ can be calculated once J_{ex} is determined. The Hartree–Fock calculation tends to overestimate the J_{ex} value greatly and gives $J_{ex}(HF)=3.54\times10^3$ cm^{-1}. Here we adopt $J_{ex} = 1.77\times10^3$ cm^{-1} by scaling down the HF value by 0.5 for the best agreement with the measured splitting of energy levels, in contrast to scaling ratio 0.6[30] and 0.67[17] used in various other places. We calculate the energy splitting of $H_{ex}(fd)$ and plot them in the third column of Fig.2. The four bands A to D in the Fig.1 can be assigned to (($^5I_8$, s_d) 17/2, t_2), (($^5I_8$, s_d) 15/2, t_2), (($^5I_7$, s_d) 15/2, t_2), (($^5I_7$, s_d) 13/2, t_2), and E is ($^5I_6$, $^2t_2$), with its tail being ($^5I_5$, $^2t_2$), where the splitting due to$H_{ex}(fd)$ are too small to be clearly distinguished. (($^5I_8$, s_d) 17/2, e) also falls in band E, but absorption to this level is spin-forbidden and so very weak. Similarly, absorption to ($^5I_4$, $^2t_2$) between bands E and F is expected to be weaker (see Table 1 for numerical results) and hence not observed in the excitation spectrum. ($^5F_5$, $^2t_2$) and (($^5I_8$, s_d) 15/2, e) are both located in broad band F as shown in Fig.1.

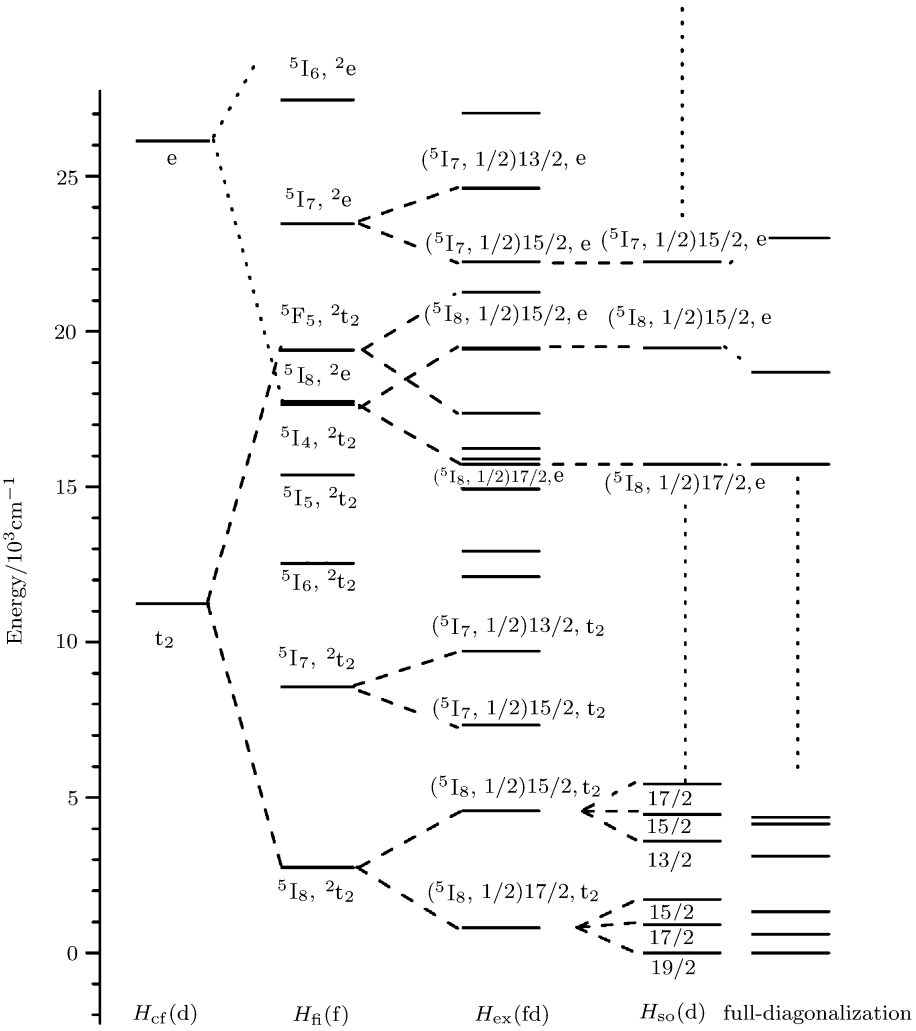


Fig.2. The energy structure for the $4f^{10}5d$ configuration of Er^{3+} in Cs_2NaYF_6 when more and more interactions are included: H_{cf} (d) (column 1) only; $H_{FI}(f) = H_{Coul}(f) + H_{so}(f)$ (column 2); Diagonal part of $H_{ex}(fd)$ (column 3); and diagonal part of $H_{so}(d)$ (column 4); full diagonalization (column 5).

Comparing their calculated absorption strengths in Table 1, we assign band F as ((^{5}I$_8$, s_d) 15/2, e) and conclude that (^{5}F$_5$, ^{2}t$_2$) is buried in band F. At the same time, band G can be simply assigned to (^{5}I$_7$, ^{2}e). From the measured excitation spectrum it can be seen that bands A and B still contain some sharp structures as shown in figure 1: 168.1 nm (A_1), 164.5 nm (A_2), 162.4 nm (A_3), 159.7 nm (B_1), 157.3 nm (B_2) and 155.5 nm (B_3). We attribute those sharp structures to the splitting of A and B by H_{so}(d). The splitting is calculated by using Eq. (11), with $\zeta_{5d} = 1.77 \times 10^3 \mathrm{cm}^{-1}$ from Ref.[17]. The result is plotted in the column 4 of Fig.2. Those states can be denoted as (((5I$_8$, s_d)17/2, l_p)19/2) (A_1), (((5I$_8$, s_d)17/2, l_p)17/2) (A_2), (((5I$_8$, s_d)17/2, l_p)15/2) (A_3), (((5I$_8$, s_d)15/2, l_p)13/2) (B_1), (((5I$_8$, s_d)15/2, l_p)15/2) (B_2) and (((5I$_8$, s_d)15/2, l_p)17/2) (B_3).

Table 1. Calculated f–d absorption line strengths (units: $|\langle 4f|r|5d\rangle|^2$) for Er^{3+} in Cs_2NaYF_6.

4f^{10}5d excited state	Line strength
(((5I$_8$, s_d)17/2, l_p)19/2) (A$_1$)	0[b]
(((5I$_8$, s_d)17/2, l_p)17/2) (A$_2$)	0.09[a]
(((5I$_8$, s_d)17/2, l_p)15/2) (A$_3$),	0.15[a]
(((5I$_8$, s_d)15/2, l_p)13/2) (B$_1$)	0.55[b]
(((5I$_8$, s_d)15/2, l_p)15/2) (B$_2$)	1.21[b]
(((5I$_8$, s_d)15/2, l_p)17/2) (B$_3$)	1.34[b]
((^{5}I$_7$, s_d) 15/2, t$_2$) (C)	0.55[c]
((^{5}I$_7$, s_d) 13/2, t$_2$) (D)	0.46[c]
(^{5}I$_6$, ^{2}t$_2$) (E);	0.23[d]
(^{5}I$_5$, ^{2}t$_2$) (buried in E)	0.02[d]
(^{5}I$_4$, ^{2}t$_2$) (not observed)	0.0003[d]
(^{5}F$_5$, ^{2}t$_2$) (buried in F)	0.75[d]
((^{5}I$_8$, s_d) 17/2, e) (not observed)	0[c]
((^{5}I$_8$, s_d) 15/2, e) (F)	2.07[c]
(^{5}I$_7$, ^{2}e) (G)	0.68[d]

Notes:

[a]The J mixing due to the non-diagonal matrix-elements of H_{so}(d) within the subspace (^{5}I$_8$, ^2l_p) is considered.

[b]Calculated by using Eq.(17) of the present work.

[c]Calculated by using Eq.(14) of Ref.[21].

[d]The sum of the two line strengths ((^{5}I$_{Jf}$, s_d)J, t$_2$) with $J = J_f - 1/2$ and $J_f + 1/2$.

To be more accurate, we calculate the splitting of the space (5I, ^{2}t$_2$) by resorting to a full diagonalization illustrated in Section 2.1. The eigenstates we are interested in, as discussed in the last paragraph, have the good quantum number J_{tp}=19/2, 17/2, 15/2, and 13/2. When $J_{tp} = 19/2$, the value for the (J_f, J) pair in the basis $|\psi\rangle$ given by Eq.(12) can only be (8, 17/2) and hence the matrix is one dimensional and diagonal; for $J_{tp} = 17/2$, there are three (J_f, J) pairs, i.e., (8, 17/2), (8, 15/2) and (7, 15/2); for $J_{tp} = 15/2$, five (J_f, J) pairs, i.e., (8, 17/2), (8, 15/2), (7, 15/2), (7, 13/2) and (6, 13/2); and for $J_{tp} = 13/2$, six (J_f, J) pairs, i.e., (8, 15/2), (7, 15/2), (7, 13/2), (6, 13/2), (6, 11/2), (5, 11/2). Hence, using Eqs.(14) and (15) we can calculate the 1×1, 3×3, 5×5 and 6×6 matrices for $J_{tp} = 19/2$, 17/2, 15/2 and 13/2, respectively. It turns out that only a small portion of the matrix elements are nonzero. The same calculation can also be done for other spectral terms of the 4f^{10} core, such as ^5F, wherever necessary. For the space (^{5}I, ^{2}e), a full diagonalization is simple and the formulae for matrix elements are given in Ref.[31].

The energies obtained by the full diagonalization are plotted in column 5 of Fig.2. It can be seen that the corrections over column 4 can be quite big. Calculations indicate that the corrections due to the non-diagonal matrix elements of H_{ex}(fd) are more important than those due to the non-diagonal matrix elements of H_{so}(d).

The isotropic electric dipole absorption line strengths starting at the 4f^{11} ground states and terminating at various 4f^{10}5d excited states can also be calculated. The results are tabulated in Table 1. Since the excitation intensities can be very different from the absorption intensities due to the efficiency of passing the absorbed energies to the emission levels or quantum efficiency, direct quantitative comparison between calculated line strengths and excitation intensity is not feasible, but the data serve as quantitative indication of the importance of the levels in the excitation spectrum.

The concept of high and low-spin 4f^{N-1}5d states for ions in the second half series of lanthanides[32] is worth remarking on here. Makhov *et al* assigned the A_1 and A_3 zero-phonon lines in the f–d excitation spectrum of Er^{3+} doped in crystal Cs_2NaYF_6[26] as SF and SA transitions, respectively. However, the calculation of the f-d excitation spectrum of Tm^{3+} doped in crystal Cs_2NaYF_6[33] shows that experimental distinction between high- and low-spin states is not always suitable, since the f–d transition intensity is not only relevant to the total spin quantum number S, but also dependent on the other quantum numbers such as L

and J. To obtain an accurate high and low-spin splitting, the percentage of low-spin ($S = 3/2$) components of the 5d excitation states needs to be calculated. The lowest four $4f^{10}5d$ excitation states (A_1, A_2, A_3 and B_1) contain 0%, 0%, 0% and 83% of low-spin components, respectively, before counting the mixing of spin due to the non-diagonal matrix-elements of $H_{so}(d)$ (or 0%, 36%, 47% and 77%, respectively, after counting the mixing). Thus, A_1 and B_1 zero-phonon lines are assigned as SF and the first SA transitions, respectively. The energy separation between high- (A_1) and low- (B_1) spin 5d levels is 3.1×10^3 cm^{-1}, similar to the HS–LS splitting observed for Er^{3+} doped in $LiYF_4$ (3.3×10^3 cm^{-1}).[17]

4. Conclusion

The energy level structure of $4f^{N-1}5d$ for heavy lanthanides occupying a six-ligand octahedral site is derived theoretically. The absorption line strengths from the ground $4f^N$ states are also given in terms of the recoupling coefficients for the angular-momentum. As an example, these results are applied to interpret the bands in the excitation spectrum of Cs_2NaYF_6:Er^{3+}. It can be seen that the theoretical results can be applied easily to any heavy lanthanide ions with the aid of the Dieke diagram and some simple numerical calculations. The high-spin and low-spin $4f^{10}5d$ states are remarked on in terms of the composition of their wavefunctions.

References

[1] Wegh R T, Donker H, Oskam K D and Meijerink A 1999 *Science* **283** 663

[2] Marsman M, Anderiessen J and van Eijk C W 2000 *Phys. Rev.* B **61** 16477

[3] Reid M F, van Pieterson L, Wegh R T and Meijerink A 2000 *Phys. Rev.* B **62** 14744

[4] van Pieterson L, Reid M F, Wegh R T, Soverna S and Meijerink A 2002 *Phys. Rev.* B **65** art. no. 045113

[5] Han B, Liang H B, Lin H H, Zhong J P, Su Q, Dorenbos P, Birowosuto M D, Zhang G B and Fu Y B 2007 *J. Appl. Phys.* **101** art. no. 113530

[6] You F T, Huang S H, Meng C X, Wang D W, Xu J H, Huang Y and Zhang G B 2007 *J. Lumin.* **122** 58

[7] Wei Z G, Sun L D, Liao C S, Jiang X C, Yan C H, Tao Y, Hou X Y and Ju X 2003 *J. Appl. Phys.* **93** 9783

[8] Zhou Y H and Lin J 2005 *J. Solid State Chem.* **178** 441

[9] Tanner P A, Mak C S K, Edelstein N M, Murdoch K M, Liu G K, Huang J, Seijo L and Barandiaran Z 2003 *J. Am. Chem. Soc.* **125** 13225

[10] Tanner P A, Mak C S K, Faucher M D, Kwok W M, Phillips D L and Mikhailik V 2003 *Phys. Rev.* B **67** 115102

[11] Song H W, Lu S Z, E S L, Gao R X, Zhang J H, Chen B J, Xia H P, Zhang J L and Ni Q H 2002 *J. Appl. Phys.* **91** 2959

[12] Xia H P, Zhang H L, Wang J H, Nie Q H and Song H W 2002 *Mater. Lett.* **53** 277

[13] Hao Z D, Zhang J H, Zhang X, Sun X Y, Luo Y S, Lu S Z and Wang X J 2007 *Appl. Phys. Lett.* **90** 261113

[14] Jia D D, Wu B Q and Zhu J 2000 *Chin. Phys.* **9** 69

[15] Guan F, Dai C J and Zhao H Y 2008 *Chin. Phys.* B **17** 3655

[16] Meng C X, Huang S H, You F T, Chang J J, Peng H S, Tao Y and Zhang G B 2005 *Acta Phys. Sin.* **54** 5468 (in Chinese)

[17] van Pieterson L, Reid M F, Burdick G W and Meijerink A 2002 *Phys. Rev.* B **65** art. no. 045114

[18] Duan C K and Reid M F 2003 *J. Solid State Chem.* **171** 299

[19] Xia S D and Duan C K 2007 *J. Lumin.* **122** 1

[20] Cowan R D 1981 *The Theory of Atomic Structure and Spectra* (Berkeley: University of California Press) p309–316

[21] Duan C K, Xia S D, Reid M F and Ruan G 2005 *Phys. Stat. Sol.* (b) **242** 2503

[22] Sugano S, Tanabe Y and Kamimura H 1970 *Multiplets of Transition-Metal Ions in Crystals* (New York-London: Academic Press) p156

[23] Ballhauson C J 1962 *Introduction to Ligand Field Theory* (London-New York: McGraw-Hill Book Company) p121

[24] Rotenberg M, Biyins R, Metropolis N and Wooten J K 1959 *The 3-j and 6-j Symbols* (Cambridge, Massachusetts: M. I. T. Press) p47–162; Alternatively, *a web-based calculator for 3j, 6j and 9j can be found* at http://plasma-gate.weizmann.ac.il/369j.html

[25] Nielson C W and Koster J F 1963 *Spectroscopic Coefficients for the p^n, d^n and f^n Configuration* (Cambridge, Massachusetts: M. I. T. Press) p6–52

[26] Makhov V N, Khaidukov N M, Lo D, Krupa J C, Kirm M and Negodin E 2005 *Opt. Mater.* **27** 1131

[27] Aull B F and Jenssen H P 1986 *Phys. Rev.* B **34** 6647

[28] Zhou X J, Tanner P A and Faucher M D 2007 *J. Phys. Chem.* C **111** 683

[29] Reid M F, van Pieterson L and Meijerink A 2002 *J. Alloys Compds.* **344** 240

[30] Burdick G W, Burdick A, Deev V, Duan C K and Reid M F 2006 *J. Lumin.* **118** 205

[31] Xia S D and Duan C K 2006 *Phys. Stat. Sol.* (b) **243** 2839

[32] Wegh R T and Meijerink A 1999 *Phys. Rev.* B **60** 10820

[33] Ma C G, Tanner P A, Xia S D and Yin M 2007 *Opt. Mater.* **29** 1620